ATP-Dependent Human Erythrocyte Glutathione-Conjugate Transporter. II. Functional Reconstitution of Transport Activity †

ARTICLE *in* BIOCHEMISTRY · APRIL 1998

Impact Factor: 3.02 · DOI: 10.1021/bi972131r · Source: PubMed

11 AUTHORS, INCLUDING:

Sanjay Awasthi
Beckman Research Institute
209 PUBLICATIONS **6,602** CITATIONS
SEE PROFILE

Sanjay K Srivastava
Texas Tech University Health Sciences Cente…
195 PUBLICATIONS **4,569** CITATIONS
SEE PROFILE

Yogesh C Awasthi
University of North Texas HSC at Fort Worth
313 PUBLICATIONS **11,331** CITATIONS
SEE PROFILE

ATP-Dependent Human Erythrocyte Glutathione-Conjugate Transporter. II. Functional Reconstitution of Transport Activity†

Sanjay Awasthi,*,‡ Sharad S. Singhal,‡ Slawomir Pikula,§ John T. Piper,|| Sanjay K. Srivastava,⊥ Robert T. Torman,‡ Joanna Bandorowicz-Pikula,§ James T. Lin,‡ Shivendra V. Singh,⊥ Piotr Zimniak,# and Yogesh C. Awasthi||

Departments of Internal Medicine and Human Biological Chemistry and Genetics, The University of Texas Medical Branch, Galveston, Texas, Department of Cellular Biochemistry, Nencki Institute of Experimental Biology, Polish Academy of Sciences, Warsaw, Poland, Mercy Hospital of Pittsburgh, Pittsburgh, Pennsylvania, and Departments of Internal Medicine and Biochemistry & Molecular Biology, University of Arkansas for Medical Sciences, and McClellan VA Hospital, Little Rock, Arkansas

Received August 27, 1997; Revised Manuscript Received February 12, 1998

ABSTRACT: Purified dinitrophenyl *S*-glutathione (DNP-SG) ATPase was reconstituted into artificial liposomes prepared from soybean asolectin. Electron micrography confirmed the formation of unilamellar vesicles with an average radius of 0.25 μm. Intravesicular volume estimated by incorporation of radiolabled inulin into the vesicles was found to be 19.7 ± 1.3 μL/mL reconstitution solution. Accumulation of the glutathione-conjugate of CDNB, DNP-SG, and of doxorubicin (DOX) in the proteoliposomes was increased in the presence of ATP as compared to equimolar ADP or adenosine 5′-[β,γ-methylene]triphosphate tetralithium. ATP-dependent transmembrane movement of DOX and DNP-SG into DNP-SG ATPase-reconstituted vesicles was saturable with respect to time, sensitive to the osmolarity of the assay medium, and temperature dependent. The energy of activation was found to be 12 and 15 kcal/mol for DNP-SG and DOX, respectively. Optimal temperature for transport was 37 °C. Saturable transport was demonstrated for DNP-SG (V_{max} of 433 ± 20 nmol/min/mg of protein, K_{mATP} = 2.4 ± 0.3 mM and $K_{mDNP-SG}$ = 36 ± 5 μM) as well as DOX (V_{max} = 194 ± 19 nmol/min/mg of protein, K_{mATP} = 2.5 ± 0.6 mM and K_{mDOX} = 2.4 ± 0.7 μM). The kinetic data for both DNP-SG and DOX transport were consistent with a random bi-bi sequential reaction mechanism. DOX was found to be a competitive inhibitor of DNP-SG transport with K_{is} of 1.2 ± 0.2 μM and DNP-SG was found to be a competitive inhibitor of DOX transport with K_{is} of 13.3 ± 2.6 μM.

Available evidence indicates heterogeneity in mechanisms mediating energy dependent efflux from mammalian cells of amphiphilic organic ions such as GS-E[1], metabolites of heme, and various pharmacologic agents (*1*−*15*). Previous studies from our laboratories have characterized a erythrocyte membrane transporter protein, DNP-SG ATPase, which catalyzed ATP hydrolysis not only in the presence of GSH conjugates (*16*), but also in the presence of chemotherapeutic drug DOX and its analogues (*6*). Incorporation of purified DNP-SG ATPase into inside-out vesicles prepared from human erythrocyte membranes enhanced the ATP-dependent uptake of DOX (*6*). Competitive inhibition of ATP-dependent DOX transport by glutathione conjugates suggested a shared mechanism for the transport of GS-E and DOX (*6*, *14*). The presence of common mechanisms for energy-dependent transport of GS-E and vincristine has subsequently been suggested in studies (*8*−*10*) investigating the functional properties of MRP (*17*), a 190 kDa glycoprotein belonging to the ATP-binding cassette (ABC) family

† This investigation was supported by NIH Grants GM32304 (Y.C.A.), CA63660 (S.A.), CA55589 (S.V.S.), and VA Merit Review (P.Z.).

* To whom all correspondence should be sent. Phone: (409) 772-6538. Fax: (409) 772-6603. E-mail: sawasthi@utmb.edu.

‡ Department of Internal Medicine, The University of Texas Medical Branch.

§ Polish Academy of Sciences.

|| Department of Human Biological Chemistry and Genetics, The University of Texas Medical Branch.

⊥ Mercy Hospital of Pittsburgh.

University of Arkansas for Medical Sciences.

[1] Abbreviations: GS-E, glutathione-electrophile conjugates; GSH, glutathione; GS-SG, glutathione-disulfide; DOX, doxorubicin (Adriamycin); DNP-SG, dinitrophenyl S-glutathione; 2-ME, 2-mercaptoethanol; MRP, multidrug resistance associated protein; MOAT, multispecific organic anion transporter; NPPB, 5-nitro-2-(3-phenylpropylamino)benzoic acid; P-gp, P-glycoprotein (*mdr*-1 gene product).

[2] The phospholipid composition of asolectin (measured by phosphorus determination) is 40 mol % PC, 33 mol % PE, 14 mol % PI, 5 mol % lysol-PC, 4 mol % cardiolipin, and 4 mol % unidentified phospholipids (*19*). Under the simplifying assumption that the MW of all the above phospholipids is the same, PC would make up 40% of the mass of the phospholipids in asolectin. Thus, if PC constitutes 17% of the total mass, phospholipids constitute 43% (by weight) of the total. Since asolectin is soluble in organic solvents, the balance is probably neutral lipids such as ergosterol (MW = 397) rather than protein, salt, water, etc. Therefore, 4 mg of asolectin would contain 1.72 mg (2.5 μmol, assuming average MW of 700) phospholipid, and 2.28 mg (5.7 μmol, assuming MW of 400) of ergosterol. The additional 1 mg of cholesterol equals 2.5 μmol. Since 1 molecule of phospholipid occupies 0.7 nm^2 and one molecule of cholesterol (and presumably ergosterol), 0.46 nm^2, 4 mg of asolectin + 1 mg of cholesterol (i.e., 2.5 × 10^{-6} mol of phospholipid and 8.2 × 10^{-6} mol of sterol) would occupy 1.05 × 10^{18} nm^2 + 2.27 × 10^{18} nm^2 = 3.32 × 10^{18} nm^2 monolayer, or 1.66 × 10^{18} nm^2 bilayer. This is 2.1 × 10^{12} vesicles if the radius is 250 nm. A similar result (2.0 × 10^{12} vesicles) is obtained under the assumption that PC makes up 17% of the asolectin, with the balance being other phospholipids with an average MW of 700.

S0006-2960(97)02131-4 CCC: $15.00
Published on Web 03/25/1998

with some homology to chloride channel proteins. Conclusive evidence, however, for the shared transport of GS-E and DOX by a single transporter is lacking due to lack of transport studies with purified transporter functionally reconstituted in artificial liposomes. In the preceding article in this issue, we have reported an improved protocol for the purification of DNP-SG ATPase to apparent homogeneity and described its kinetic properties. In this communication, we report the functional reconstitution of purified DNP-SG ATPase and demonstrate that reconstituted DNP-SG ATPase can mediate ATP-dependent transport of DNP-SG as well as DOX. Kinetic properties of this transporter as determined in proteoliposomes are described, and the possible physiological role of the protein is discussed.

EXPERIMENTAL PROCEDURES

Reagents. [^{3}H]DNP-SG was enzymatically synthesized, purified and authenticated as described by us previously (6). [Carboxyl-^{14}C]inulin was purchased from ICN Radiochemicals (Irvine, CA). Soybean asolectin (17% w/w phosphatidyl choline, cat. no. P-5638) was purchased from Sigma (St. Louis, MO). Sources of other chemicals used in these studies have been described in the preceding article in this issue.

Reconstitution of DNP-SG ATPase into Liposomes. Reconstitution of DNP-SG ATPase was performed using methods similar to those previously used by us for functional reconstitution of rat liver canalicular MOAT (*18*). Purified DNP-SG ATPase was dialyzed overnight against a buffer containing 10 mM Tris-HCl, pH 7.4, 2 mM $MgCl_2$, 1 mM EGTA, 100 mM KCl, 40 mM sucrose, 2.8 mM 2-ME and 0.025% (v/v) polidocanol (reconstitution buffer). One milliliter of an aqueous emulsion of untreated soybean asolectin (40 mg/mL) and cholesterol (10 mg/mL) was prepared in the reconstitution buffer by sonication, and a 100 μL aliquot of this emulsion was added to a 0.9 mL aliquot of dialyzed DNP-SG ATPase containing 1−10 μg of protein. The reaction mixture was sonicated for 15 s at 50 W, after which 200 mg SM-2 Biobeads preequilibrated in the reconstitution buffer (without polidocanol) were added to initiate vesiculation by removal of detergent. After incubation for 4 h at 4 °C, SM-2 Biobeads were removed by centrifugation at 3620*g*.

Transport Studies. Composition of the transport buffer was identical to that of the reconstitution buffer except that polidocanol was omitted. Reconstituted proteoliposomes were diluted 2−20-fold in 90 μL of transport buffer containing either [^{3}H]DNP-SG (1.87×10^4 cpm/nmol) or 14-[^{14}C]DOX (8.9×10^4 cpm/nmol) and incubated for 15 min at 37 °C. DOX concentrations from 2 to 6 μM and DNP-SG concentrations from 14 to 170 μM were used. Measurement of ATP-dependent transport was initiated by addition of 10 μL of ATP prepared in transport buffer to the experimental group and 10 μL of transport buffer alone to the control. The final concentration of ATP in different experiments ranged between 1 and 10 mM. After incubation with ATP for 1−20 min, aliquots of the reaction mixtures containing 2−20 ng of reconstituted protein were filtered using a Millipore multiscreen 96 well plate vacuum filtration system as previously described (*6*). The filtration membranes were individually cut out of the filtration manifold and solubilized in scintillation cocktail overnight before radioactivity counting.

Background binding of the radiolabeled-substrate to the filtration membrane was determined for each experimental condition and subtracted to obtain the vesicular uptake of substrate. The effect of DNP-SG ATPase on substrate uptake by vesicles was studied by comparing uptake with or without ATP by liposomes prepared exactly as described above, except without addition of DNP-SG ATPase. Possible nonspecific effects of nucleotides on substrate uptake by the vesicles were studied by substituting equal concentration of ADP or methylene-ATP for ATP in the controls. Also, the possible osmotic effects of ATP addition were investigated by substituting equiosmolar NaCl solutions for ATP in controls.

Substrate Kinetics. ATP-dependent DNP-SG transport kinetics were evaluated at DNP-SG concentrations from 14 to 170 μM and ATP concentrations between 1 and 10 mM. ATP-dependent DOX transport kinetics were performed at DOX concentrations from 2 to 6 μM and ATP concentrations from 1 to 10 mM. The average ATP-dependent velocity of uptake obtained from measurement at 5 min after addition of ATP was taken as the initial velocity since preliminary studies indicated that the uptake of both DOX and DNP-SG was approximately linear within this period. Using a quasi-Newton algorithm for nonlinear estimation in the Statistica software package, the initial velocity data were analyzed by fitting the rate equation for equilibrium ordered or random bi-bi sequential reaction mechanisms (eqs 1 and 2, respectively), where v is the observed initial velocity, V_{max} is the

$$v = \frac{V_{max}AB}{(K_{mB}A) + (K_{iA}K_{mB}) + (AB)} \quad (1)$$

$$v = \frac{V_{max}AB}{(K_{mB}A) + (K_{mA}B) + (K_{iA}K_{mB}) + (AB)} \quad (2)$$

predicted maximal velocity, A and B are concentrations of substrates, K_{mA} and K_{mB} are the respective K_m values, and K_{iA} is the rate constant for binding of substrate A.

Inhibition Kinetics. Initial velocity measurements for DOX transport were performed using 14-[^{14}C]DOX concentrations from 2 to 6 μM and DNP-SG concentrations from 12.5 to 75 μM. Initial velocity measurements were performed at [^{3}H]DNP-SG concentrations from 14 to 170 μM and DOX concentrations from 1 to 7.5 μM. Using a quasi-Newton method for nonlinear estimation in the Statistica software package, the initial velocity data were analyzed by fitting equations for uncompetitive, competitive, or noncompetitive inhibition (eqs 3−5, respectively), where v is the

$$v = \frac{V_{max}S}{K_m + S\left[1 + \left(\frac{I}{K_{ii}}\right)\right]} \quad (3)$$

$$v = \frac{V_{max}S}{K_m\left[1 + \left(\frac{I}{K_{is}}\right)\right] + S} \quad (4)$$

$$v = \frac{V_{max}S}{K_m\left[1 + \left(\frac{I}{K_{is}}\right)\right] + S\left[1 + \left(\frac{I}{K_{ii}}\right)\right]} \quad (5)$$

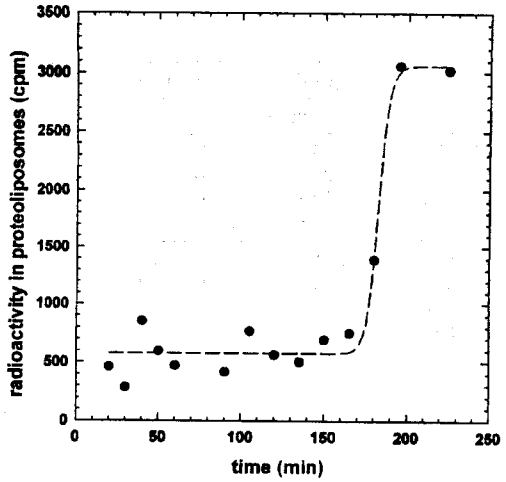

FIGURE 1: Time course of vesiculation during reconstitution of DNP-SG ATPase. The time course of vesiculation was studied by including [^{14}C]inulin (513 ± 18 cpm/μL) in the reconstitution buffer containing 5 μg DNP-SG ATPase/mL. Aliquots of the reconstitution solution were taken at specified times after addition of SM-2 biobeads. Vesicles were separated from free inulin by passing vesicles over columns of Sephadex G-50 prepared in 1 mL syringes and collecting the vesicles in the void volume.

observed initial velocity, V_{max} is the predicted maximal velocity, A and B are concentrations of substrates, K_m is that of the transported substrate, I is inhibitor concentration, and K_{is} and K_{ii} are the binding constants for the inhibitor with either the enzyme or the enzyme−substrate complex, respectively.

RESULTS

Characterization of DNP-SG ATPase Reconstituted Liposomes. A plot of vesicle associated radioactivity of [^{14}C]-inulin vs time after initiating reconstitution indicated that vesiculation was essentially complete after 4 h (Figure 1). Assuming that the majority of vesicle-associated inulin was present inside vesicles, the amount of entrapped inulin indicated an intravesicular volume of 19.7 ± 1.3 (n = 3) μL/mL reaction mixture. Electron micrography of the 104000g pellet of the vesiculation reaction mixture revealed the formation of primarily unilamellar vesicles with an average radius of 249 ± 99 nm [range 61−607 nm, median 242 nm (n = 100)] (Figure 2). The volume of an average vesicle calculated from the radius was 6.5 × 10^{-11} μL. From these results, the estimated number of vesicles/mL reaction mixture was about 3 × 10^{11}. These results were in general agreement with the maximal number of 2 × 10^{12} vesicles estimated from the amount of phospholipid and cholesterol used for reconstitution.[2] Assuming complete incorporation of DNP-SG ATPase and assuming that 38 000 Da is an accurate estimate of its molecular mass, reconstitution with purified DNP-SG ATPase should yield a maximum of 53 molecules of DNP-SG ATPase/vesicle in a reconstitution that contains 1 μg of protein. For the studies of ATP-dependent transport of DNP-SG and DOX described below, proteoliposomes were prepared in reconstitution buffer containing 1−10 μg of protein, 1 mg of cholesterol, and 4 mg of phosphatidylcholine/mL. Vesicles prepared under the same conditions without addition of DNP-SG ATPase (liposomes) were used as no-protein controls.

Effect of ATP on DNP-SG or DOX Uptake by Liposomes and Proteoliposomes. Proteoliposomes used for these studies

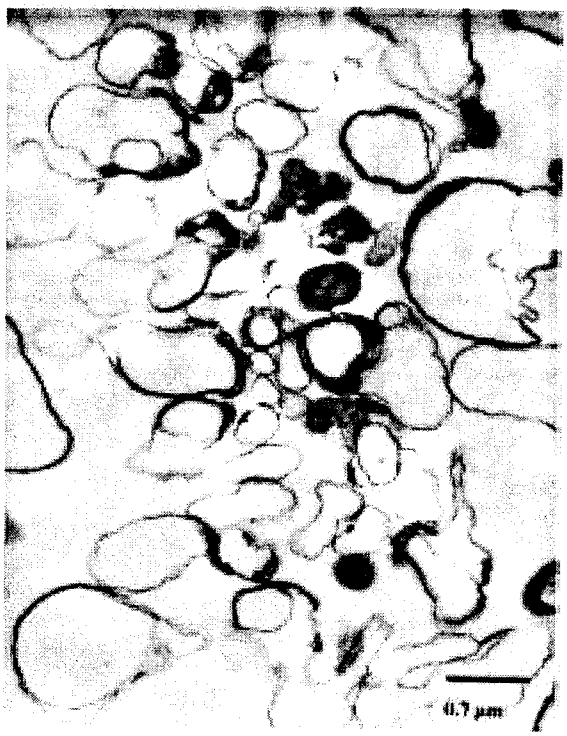

FIGURE 2: Electron Micrograph of proteoliposomes reconstituted with DNP-SG ATPase. Vesicles were prepared as described in Experimental Procedures. An 18150× magnified electron micrograph is presented.

prepared with a fixed protein/lipid ratio of 3 μg of protein/5 mg of lipid (0.6 μg of protein/mg of lipid) (Table 1). The background binding to the filter obtained by omitting liposomes and proteoliposomes from the transport reaction mixture was found to be relatively high, but quite reproducible under present conditions (Table 1). Background binding of both DNP-SG and DOX was similar when either NaCl, ADP, met-ATP or ATP was added to the transport buffer. ATP-independent uptake of DNP-SG and DOX by either liposomes (without DNP-SG ATPase) or proteoliposomes (with DNP-SG ATPase) obtained by subtracting the corresponding background was found to be similar in the presence of NaCl, ADP, or met-ATP (Figure 3). Uptake of DNP-SG by liposomes was not increased by ATP, whereas uptake of DNP-SG in proteoliposomes after 5 min in the presence of ATP, 20.9 pmol/5 min, was more than 10-fold greater than the average of all other groups, 1.3 ± 0.3 pmol (p < 0.0001) (Figure 3A). In contrast to DNP-SG, presence of ATP significantly increased the uptake of DOX by liposomes as compared with uptake observed in the presence of either NaCl, ADP, or ATP (9.3 pmol vs an average of 6.1 for the other three groups) (Figure 3B). This presumed nonspecific effect of ATP on DOX uptake by liposomes (3.2 pmol) was relatively minor (approximately one-fifth) compared to specific, ATP-dependent DOX transport into proteoliposomes (20.1 pmol). Specific ATP-dependent rates of uptake of DNP-SG and DOX were found to 87 and 59 nmol/min/mg of protein, respectively.

Time dependence of ATP-Dependent Uptake of DNP-SG and DOX by Proteoliposomes. For these studies, the amount of protein used for reconstitution was increased 3-fold to 9 μg/mL (protein/lipid ratio of 1.8 μg/mg). Uptake of DNP-SG or DOX by proteoliposomes was measured with respect

Table 1: Effect of ATP on DNP-SG or DOX Uptake by Proteoliposomes[a]

	[^{3}H]DNP-SG retained by filter (pmol)			14-[^{14}C]DOX retained by filter (pmol)		
	background	liposomes	proteoliposomes	background	liposomes	proteoliposomes
NaCl	60.8 ± 0.2	62.0 ± 0.8 (1.2)[b]	62.2 ± 0.5 (1.4)	14.1 ± 0.3	20.5 ± 0.3 (6.4)	19.9 ± 0.3 (5.8)
ADP	61.1 ± 0.2	62.3 ± 0.4 (1.1)	62.2 ± 0.2 (1.1)	14.5 ± 0.2	20.5 ± 0.1 (6.0)	21.2 ± 0.2 (6.7)
Met-ATP	60.8 ± 0.8	62.4 ± 0.5 (1.6)	62.3 ± 0.4 (1.5)	13.9 ± 0.1	19.8 ± 0.3 (5.9)	20.8 ± 0.5 (6.9)
ATP	60.9 ± 1.4	62.7 ± 0.6 (1.8)	81.8 ± 0.9 (20.9)	13.6 ± 0.3	22.8 ± 0.2 (9.3)	33.7 ± 0.4 (20.1)

[a] Proteoliposomes were prepared, as described in Experimental Procedures, in the presence of 3 μg of purified DNP-SG ATPase and 5 mg of lipid/mL (protein/lipid ratio of 0.6 μg of protein/mg of lipid). Liposomes were prepared in an identical manner except that DNP-SG ATPase was omitted. The transport reaction mixture, containing 2.5 mg/mL lipid (corresponding to 1.5 μg of protein/mL for the proteoliposomes) and either 100 μM [^{3}H]DNP-SG (sp. act. 18.7 cpm/pmol) or 3.6 μM 14-[^{14}C]DOX (sp. act. 89 cpm/pmol), was allowed to equilibrate at 37 °C for 10 min. Liposomes and proteoliposomes were omitted for determination of background binding to the filter. Measurement was initiated upon addition of either 4 mM ADP, 4 mM met-ATP or 4 mM ATP or 6 mM NaCl. Aliquots of reaction mixtures containing 75 μg of lipid (corresponding to 45 ng of protein for proteoliposomes) were filtered. Average ± sd of triplicate determinations are presented. [b] Uptake obtained by subtracting the corresponding background.

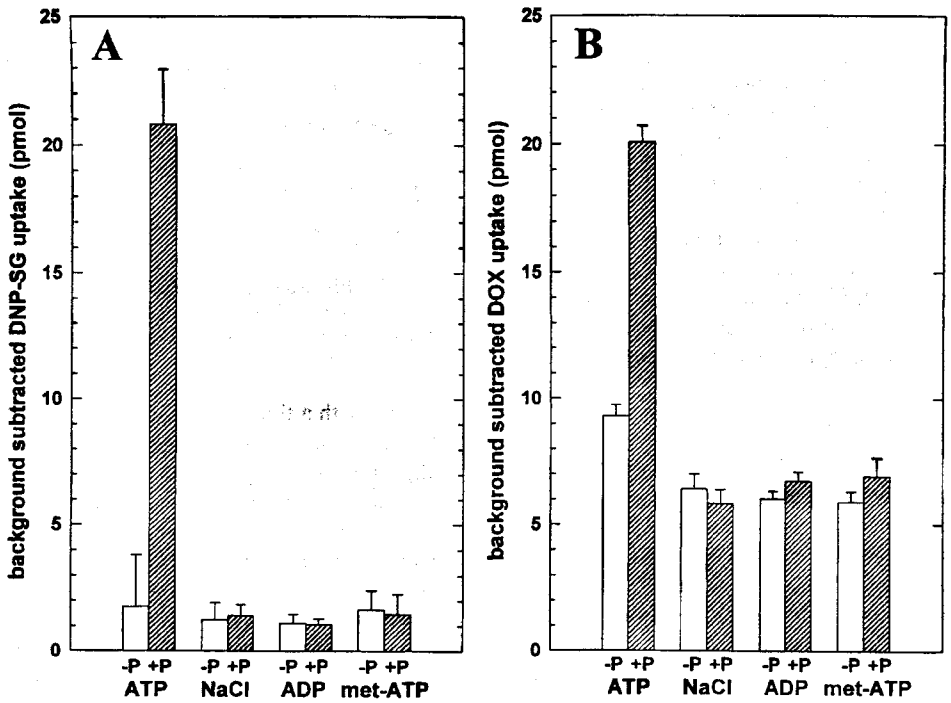

FIGURE 3: Background subtracted DNP-SG and DOX uptake by liposomes and proteoliposomes. Uptake by liposomes or proteoliposomes of [^{3}H]DNP-SG (sp. act. 1.87 × 10^4 cpm/nmol) (panel A), or 14-[^{14}C]DOX (sp. act. 8.9 × 10^4 cpm/nmol) (panel B) was compared in the presence of NaCl, ADP, methylene-ATP, or ATP. Proteoliposomes used for these studies were reconstituted with 3 μg of protein and 5 mg of lipid/mL reconstitution buffer (protein/lipid ratio 0.6 μg/mg). Protein was omitted for reconstitution of liposomes. Liposomes or proteoliposomes were diluted 2-fold in transport buffer containing 100 μM [^{3}H]DNP-SG or 3.6 μM 14-[^{14}C]-DOX. After equilibration at 37 °C for 10 min, transport was initiated by addition of either 6 mM NaCl or an equiosmolar amount (4 mM) of each nucleotide. Aliquots of transport buffer (30 μL) were filtered in triplicate after 5 min and radioactivity remaining on the nitrocellulose filter of each well in the 96 well plate was quantified. Background binding of DNP-SG and DOX to the filtration membrane was determined by filtering transport buffer containing 100 μM DNP-SG or 3.6 μM DOX without either liposomes or proteoliposomes, and containing NaCl or respective nucleotide. Data are presented in terms of uptake delta pmol/5 min (n = 3). Open bars (−P) represent liposomes while shaded bars (+P) represent proteoliposomes reconstituted with DNP-SG ATPase.

to time in the presence of either 4 mM ADP, methylene-ATP, ATP, or 6 mM NaCl (Figure 4,panels A and B, respectively). ATP-dependent uptake calculated by subtracting uptake observed in the presence of either NaCl, ADP, or met-ATP are also presented (Figure 4 panels A and B, inset). Uptake of DNP-SG or DOX by proteoliposomes was not significantly different whether NaCl, ADP, or met-ATP was included in the transport buffer. Uptake of DNP-SG and DOX was significantly greater when 4 mM ATP was included. ATP-dependent uptake was calculated by subtracting out the uptake in proteoliposmes in absence of ATP (Figure 4 panels A and B, insets). Nonlinear regression analysis of ATP-dependent uptake of DNP-SG yielded an apparent rate constant of 4.8 min^{-1}, and maximal ATP-dependent DNP-SG uptake of 69.8 pmol were also similar. The corresponding rate constant and maximal uptake for DOX were 2.2 min^{-1} and 38.4 pmol, respectively. ATP-dependent uptake values for DNP-SG and DOX extrapolated from regression at 5 min (43.2 and 34.4 pmol) were 2.3 and 2.5-fold higher than specific ATP-dependent uptake observed in proteoliposomes reconstituted with only 3 μg of protein/mL reconstitution buffer. These results suggested that ATP-dependent transport was roughly linear with respect to the amount of protein used for reconstitution.

ATP-Dependent Transmembrane Gradient in DNP-SG ATPase Reconstituted Liposomes. If we assume negligible

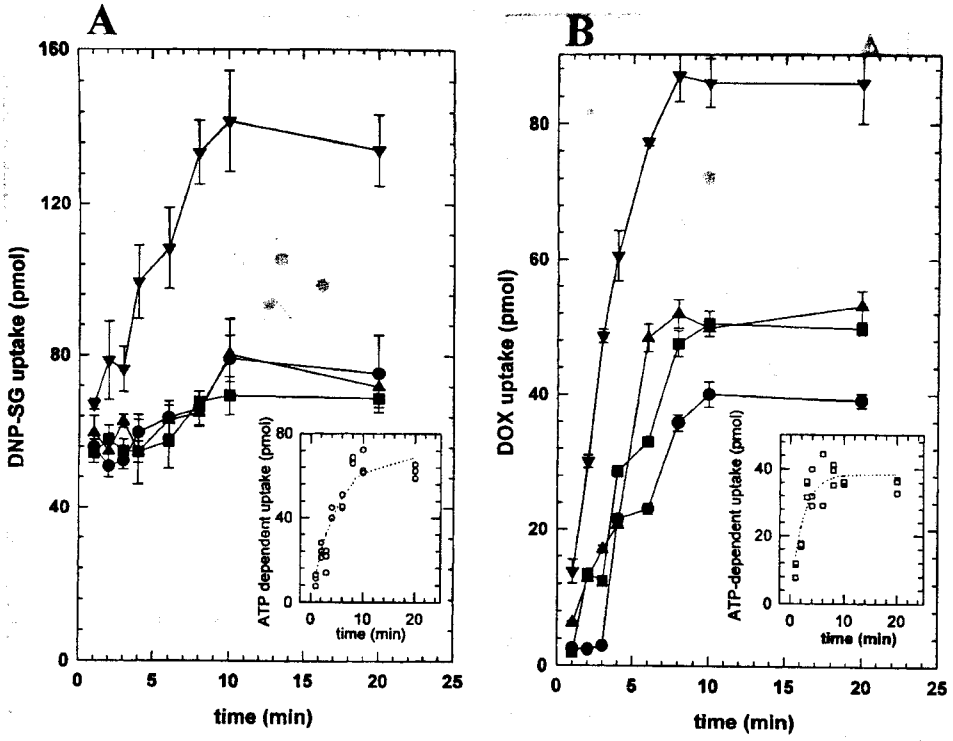

FIGURE 4: Time dependence of DNP-SG and DOX uptake in proteoliposomes. Proteoliposomes reconstituted in the presence of 9 μg DNP-SG ATPase protein/mL (protein/lipid ratio of 1.8 μg/mg) were diluted 2-fold in transport buffer containing 100 μM [^{3}H]DNP-SG (panel A) or 3.6 μM 14-[^{14}C]-DOX (panel B). After equilibration at 37 °C for 10 min, transport was initiated by addition of either 4 mM ADP (■), met-ATP (▲), ATP (▼), or 6 mM NaCl (●). Aliquots of transport buffer (30 μL) were filtered in triplicate after varying incubation times and radioactivity remaining on the nitrocellulose filter of each well in the 96 well plate was quantified. ATP-dependent uptake of DNP-SG (○) and DOX (□) (insets, panels A and B, respectively) was determined by subtracting uptake observed at 5 min after addition of either ADP, metATP, or NaCl from uptake observed 5 min after addition of ATP. Points are average of three determinations each performed in triplicate. The regression curves presented were derived by fitting to the Boltzmann equation.

membrane binding, the average ATP-independent DNP-SG uptake by vesicles (1.32 ± 0.22 pmol) corresponds to an intravesicular concentration of 5.5 ± 1 μM in the absence of ATP. However, the amphiphilic nature of DNP-SG indicates that a significant amount of it may be membrane associated. We thus estimated the membrane-bound fraction by measuring ATP-dependent uptake at varying osmolarity (Figure 5). Membrane-bound DNP-SG was estimated at 1.1 ± 2.2 pmol/mg of lipid. An intravesicular DNP-SG concentration of approximately 1 μM could be estimated from these results. The intra/extravesicular concentration ratio near 0.05 in the absence of ATP indicated that the vesicles used for these studies were relatively impermeable to DNP-SG. In contrast, intravesicular DNP-SG concentration in proteoliposomes reconstituted with 3 μg of protein/mL after 5 min in the presence of ATP was 76 ± 9 μM, corresponding to an intra/extravesicular concentration ratio of 0.76. These results indicated that although the presence of ATP increased the vesicular accumulation of DNP-SG, the intra/extravesicular concentration gradient remained less than 1 within 5 min under conditions of these experiments (Figure 3A). The maximal ATP-dependent uptake of DNP-SG obtained from studies with proteoliposomes reconstituted with 9 μg/mL purified DNP-SG ATPase (Figure 4A) corresponds to an intravesicular concentration of 227 ± 14 μM, an intra/extravesicular gradient of 2.27-fold. This concentration is over 40-fold higher than the intravesicular concentration in the absence of ATP (<5.5 μM). Results of these studies demonstrate that DNP-SG ATPase can mediate energy dependent transport against a concentration gradient.

Nonspecific binding of DOX to the proteoliposome (4.7 ± 1.1 pmol) was significantly greater than that observed for DNP-SG (Figure 5B). Subtracting this value from the average ATP-independent uptake of DOX in liposomes or proteoliposomes (6.3 ± 1.1), we obtained 1.6 pmol as the approximate intravesicular uptake of DOX. This corresponds to 5 μM, roughly equal to the extravesicular concentration of 4 μM. The average ATP-dependent maximal uptake from regression analysis of data for time-dependent DOX uptake 38.4 ± 2.4 pmol corresponded to an intravesicular concentration of 114 μM. The approximate intra/extravesicular DOX concentration gradient was greater than 20, indicating the presence of an active transport mechanism for DOX.

Temperature Dependence of DNP-SG and DOX Transport. ATP-dependent transport was found to be optimal near 37 °C for both DNP-SG and DOX (Figure 6). Decline in transport activity at higher temperature suggested a heat labile nature of the transporter. The activation energies for DNP-SG and DOX transport calculated according to the Arrhenius equation were 12 and 15 kcal/mol, respectively. Taken together, these results indicate that at physiologic temperature, DNP-SG ATPase can transport DNP-SG and DOX across membranes against a concentration gradient.

Effect of GSH, GS-SG, and NPPB on DNP-SG and DOX Transport. Because GSH appears to stimulate transport functions of MRP (*9*, *20*), we examined the effect of GSH or GSSG on DNP-SG and DOX transport (Figure 7). Statistically significant, although relatively minor (approximately 25%), inhibition of DNP-SG and DOX transport was observed only at 1000 μM GSH or GS-SG ($n = 3, p < 0.01$).

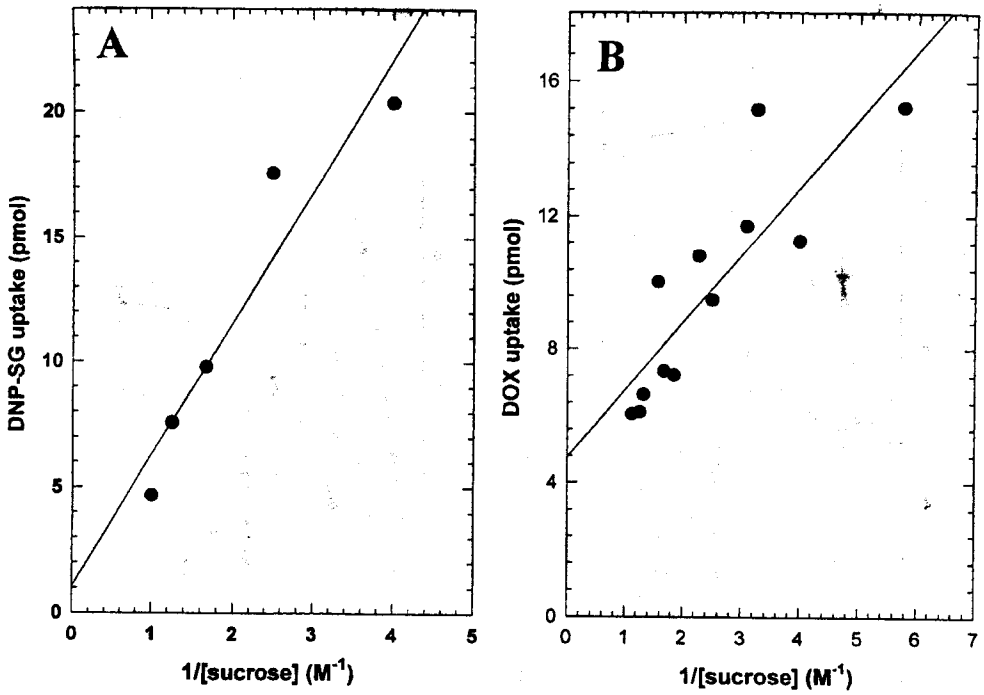

FIGURE 5: Osmolar sensitivity of ATP-dependent DNP-SG and DOX uptake. Proteoliposomes reconstituted with 3 μg of DNP-SG ATPase protein/mL (protein/lipid ratio of 0.6 μg/mg) were diluted 2-fold in transport buffer containing 100 μM [^{3}H]DNP-SG (panel A) or 3.6 μM 14-[^{14}C]-DOX (panel B) along with sucrose (between 0.25 and 1 M). After equilibration at 37 °C for 10 min, transport was initiated by addition of either 4 mM ATP or 6 mM NaCl. Aliquots of transport buffer (30 μL) were filtered in triplicate after 5 min, and radioactivity remaining on the nitrocellulose filter of each well in the 96 well plate was quantified. ATP-dependent uptake of DNP-SG and DOX was determined by subtracting uptake observed at 5 min after addition of 6 mM NaCl from uptake observed 5 min after addition of 4 mM ATP. Linear regression was used to extrapolate uptake at infinite sucrose concentration. Points represent averages of three determinations performed in duplicate. Standard deviations were less than 10%.

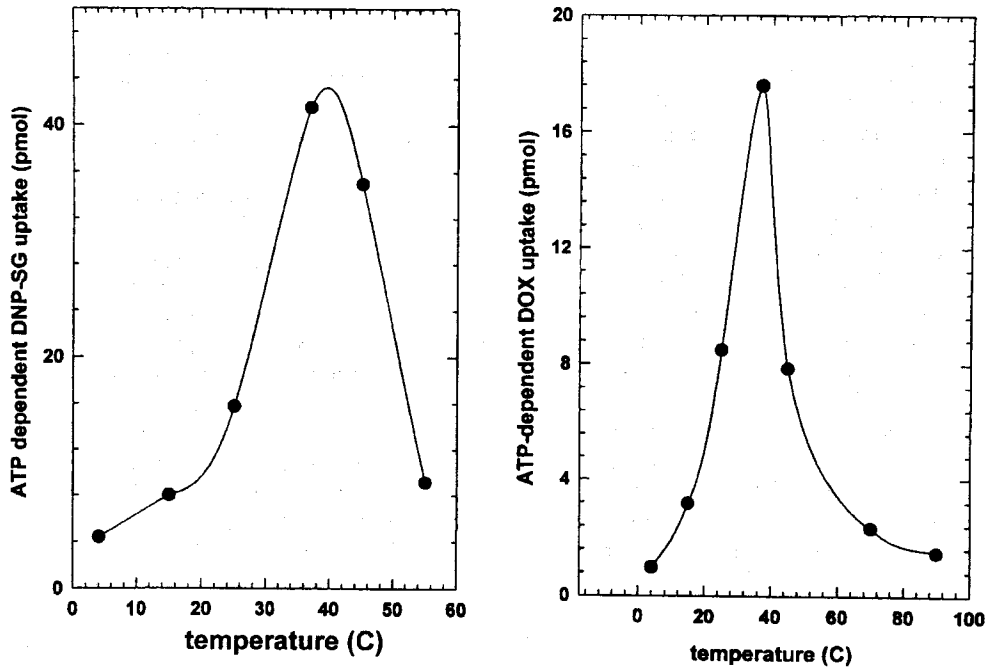

FIGURE 6: Temperature dependence of DNP-SG and DOX transport by proteoliposomes. Proteoliposomes reconstituted with 3 μg DNP-SG ATPase protein/mL (protein/lipid ratio of 0.6 μg/mg) were diluted 2-fold in transport buffer containing 100 μM [^{3}H]-DNP-SG or 3.6 μM 14-[^{14}C]-DOX. After equilibration at temperatures ranging from 4 to 90 °C for 10 min, transport was initiated by addition of either 4 mM ATP or 6 mM NaCl. Aliquots of transport buffer (30 μL) were filtered in triplicate after 5 min, incubation at the respective temperature. Radioactivity remaining on the nitrocellulose filter of each well in the 96 well plate was quantified. ATP-dependent uptake of DNP-SG and DOX was determined by subtracting uptake observed at 5 min after addition of 6 mM NaCl from uptake observed 5 min after addition of 4 mM ATP. The points represent means of triplicate measurements in a single experiment with standard deviations less than 5%.

These results suggested that GSH at physiologically relevant concentrations (1−2 mM) would have a weak inhibitory effect, while GSSG levels prevalent in cells (<50 μM) would have no significant effect on the transport activity of the

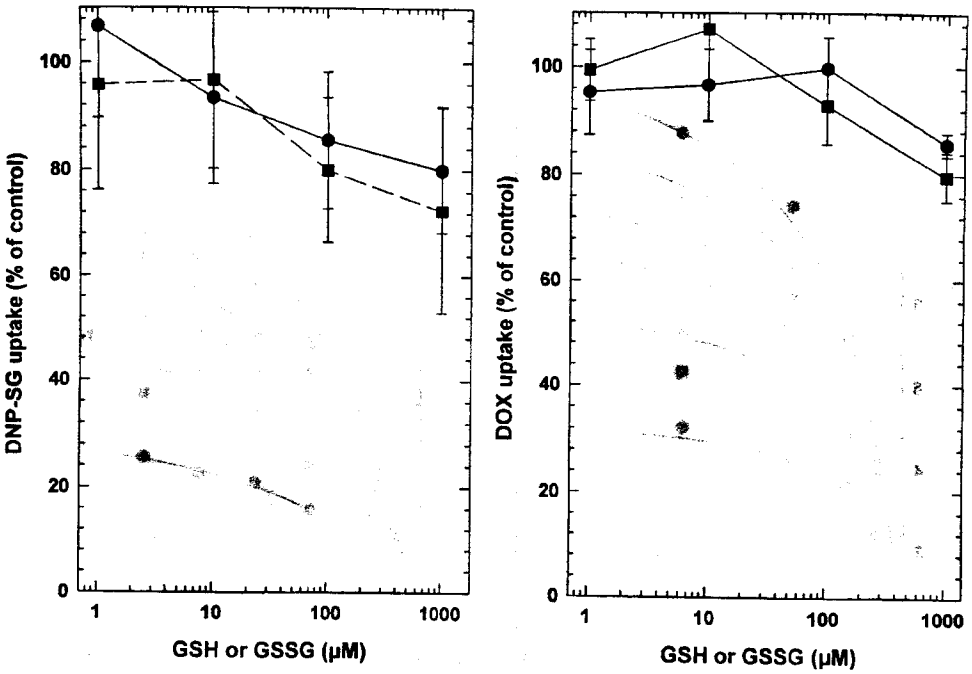

FIGURE 7: Effect of GSH or GSSG on DNP-SG and DOX transport by proteoliposomes. Proteoliposomes reconstituted with 3 μg of DNP-SG ATPase protein/mL (protein/lipid ratio of 0.6 μg/mg) were diluted 2-fold in transport buffer containing 100 μM [^{3}H]DNP-SG or 3.6 μM 14-[^{14}C]DOX as well as 0−1000 μM GSH (●) or GSSG (■). After equilibration at 37 °C for 10 min, transport was initiated by addition of either 4 mM ATP or 6 mM NaCl. Aliquots of transport buffer (30 μL) were filtered in triplicate after 5 min. Radioactivity remaining on the nitrocellulose filter of each well in the 96 well plate was quantified. ATP-dependent uptake of DNP-SG and DOX was determined by subtracting uptake observed at 5 min after addition of 6 mM NaCl from uptake observed 5 min after addition of 4 mM ATP. Points represent average of triplicate measurements in a single experiment.

DNP-SG ATPase. Since increased chloride channel activity has been observed in MDR transfected cells (*7*), we investigated the effect of NPPB, a relatively nonspecific chloride channel inhibitor on DNP-SG and DOX transport. No inhibition of DNP-SG or DOX transport was observed when 100 μM NPPB was included in the transport medium (activity 103 ± 6% and 108 ± 4% of control, $n = 3$). These results indicated that any chloride channel function of DNP-SG ATPase (or copurified proteins) was not a significant contributor to DNP-SG transport.

Kinetic Properties of DNP-SG Transport with Respect to DNP-SG and ATP. Since time-dependence experiments indicated approximate linearity of DNP-SG transport rate within the first 5 min, this time point was chosen for measurements of initial velocity for kinetic studies. DNP-SG uptake was determined in proteoliposomes as well as liposomes at 5 min after addition of ATP with concentration of DNP-SG varying from 14 to 170 μM and of ATP from 1 to 10 mM. ATP-dependent uptake in liposomes was subtracted from that observed in proteoliposomes. The observed initial velocities were analyzed by nonlinear regression fitting equations for equilibrium ordered (eq 1) or sequential (eq 2) mechanisms. Fitting the equilibrium-ordered equation yielded a reduced χ^2 value of 3757, whereas the sequential equation yielded a reduced χ^2 of 642. The observed values and theoretical curves obtained from fitting the random bi-bi sequential model equation are presented (Figure 8A). These results demonstrated saturable transport of DNP-SG with respect to ATP and DNP-SG (K_{mATP} = 2.4 ± 0.3 mM, $K_{mDNP-SG}$ = 36 ± 5 μM). The theoretical V_{max} (normalized to milligrams of purified DNP-SG ATPase) was found to be 433 ± 20 nmol/min/mg of of protein, n = 25). The maximal velocity of DNP-SG stimulated ATP-hydrolysis determined at a fixed ATP concentration of 1.6 mM (see Table 2 of the preceding article in this issue) was 416 nmol/min/mg of protein. Using the K_m for ATP of 2.4 mM determined in the present studies, maximal velocity of DNP-SG ATPase activity at infinite ATP concentration would be 1040 nmol/min/mg of protein. Maximal initial velocity for DNP-SG transport is expected to be half of this value, assuming that 50% of the protein is incorporated in the proper orientation for transport. The observed V_{max} for DNP-SG transport in the expected range suggests a 1:1 stoichiometry between ATP-hydrolysis and DNP-SG transport. Assuming that DNP-SG ATPase was the only transporter, an apparent turnover number of 0.27 s^{-1} was calculated using 38 kDa as the molecular mass. If a random orientation of the protein in the reconstituted membrane is assumed, the turnover number would double to 0.54 s^{-1}.

Kinetic Properties of DOX Transport with Respect to ATP. DOX uptake was determined in proteoliposomes as well as liposomes at 5 min after addition of ATP with concentration of DOX varying from 2 to 6 μM and of ATP from 1 to 10 mM. ATP-dependent uptake in liposomes (no DNP-SG ATPase present during vesiculation) was subtracted from that observed in proteoliposomes (DNP-SG ATPase present during vesiculation). Equations for equilibrium ordered or random bi-bi sequential reaction mechanisms (eqs 1 and 2) were fitted to initial velocity measurements of ATP-dependent DOX transport. A reduced χ^2 value of 247 was obtained from the equilibrium-ordered equation as compared with 72 obtained with the sequential equation. The observed values and theoretical curves obtained from fitting the random bi-bi sequential model equation are presented (Figure 8B). Saturable transport of DOX was observed with respect to ATP and DOX (K_{mATP} = 2.5 ± 0.6 mM, K_{mDOX} = 2.4 ±

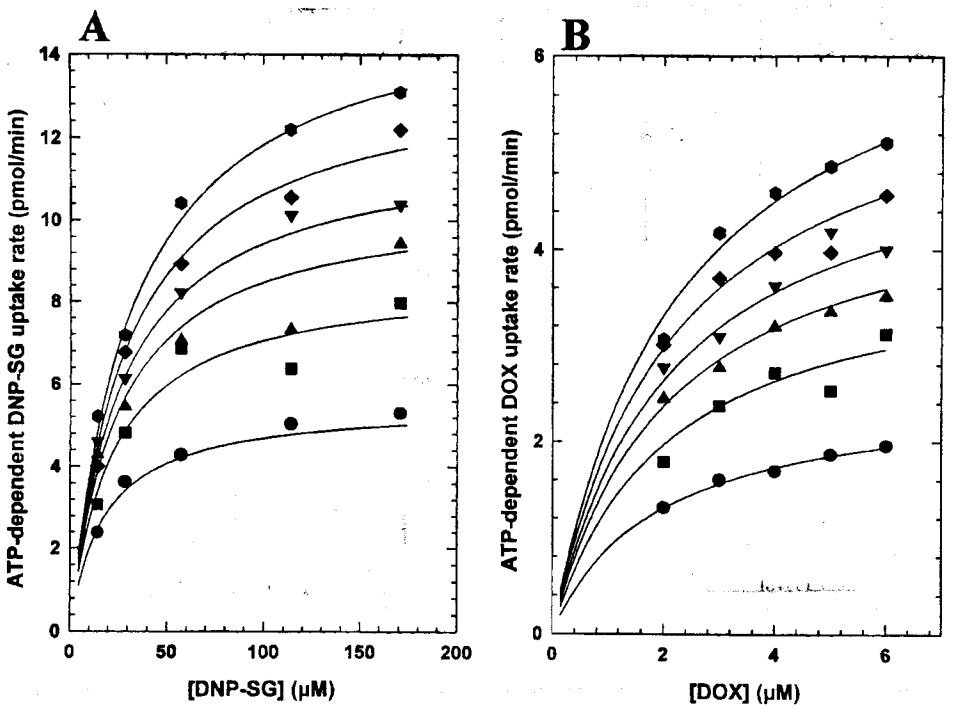

FIGURE 8: Kinetics of ATP-dependent DNP-SG and DOX transport with respect to varying DNP-SG and ATP. Proteoliposomes reconstituted with 3 μg of DNP-SG ATPase protein/mL (protein/lipid ratio of 0.6 μg/mg) were diluted 2-fold in transport buffer containing 14, 28, 57, 114, and 170 μM [^{3}H]DNP-SG (panel A) or 2, 3, 4, 5, and 6 μM 14-[^{14}C]DOX (panel B). Final ATP concentrations in the transport buffers were 1 (●), 2 (■), 3 (▲), 4 (▼), 6 (◆) and 10 (⬢) mM. After equilibration at 37 °C for 10 min, transport was initiated by addition of either ATP or equiosmolar NaCl. Aliquots of transport buffer (30 μL) were filtered in triplicate after 5 min. Radioactivity remaining on the nitrocellulose filter of each well in the 96 well plate was quantified. ATP-dependent uptake of DNP-SG and DOX was calculated by subtracting uptake in the presence of NaCl from that observed in the presence of ATP. Points represent average of triplicate determinations with standard deviations less than 5%. The theoretical lines were generated using a quasi-Newton algorithm in Statistica for nonlinear regression to fit the equation for a random bi-bi sequential reaction mechanism (eq 2) to the data.

0.7 μM, and V_{max} = 194 ± 19 nmol/min/mg of protein, n = 25). The maximal velocity of DOX-stimulated ATP hydrolysis determined at a fixed ATP concentration of 1.6 mM (see Table 2 of the preceding article in this issue) was 230 nmol/min/mg of protein. Using the K_m for ATP of 2.5 mM determined in the present studies, maximal velocity of DOX-stimulated ATPase activity at infinite ATP concentration would be 589 nmol/min/mg of protein. Maximal initial velocity for DOX transport was expected to be half of this value, assuming incorporation of half of the protein in the proper orientation for transport. The observed V_{max} for DOX transport in the expected range suggests a 1:1 stoichiometry between ATP-hydrolysis and DOX transport.

Inhibition of DNP-SG Transport by DOX. Initial velocity of transport was estimated by measuring ATP-dependent DNP-SG uptake at 5 min at five concentrations of DNP-SG between 14 and 170 μM and four concentrations of DOX between 1 and 5 μM. Fitting the three variable equation for uncompetitive inhibition (eq 3) yielded a K_{ii} of 2.9 ± 0.5 μM and reduced χ^2 value of 1935, whereas fitting for competitive inhibition (eq 4) yielded a K_{is} of 1.2 ± 0.2 μM and reduced χ^2 value of 806. Fitting the four variable noncompetitive inhibition (eq 5) yielded K_{is} of 1.9 ± 0.5 μM, K_{ii} of 12.5 ± 6.5 μM, and reduced χ^2 of 503. An F test for incremental sum of squares indicated that the precision of the present studies did not justify the inclusion of the additional variable in the analysis (*21*). Eadie-Hofstee plots of the activity data and the theoretical model for competitive inhibition are presented (Figure 9A). These results indicated that inhibition of DNP-SG transport by DOX was more likely due to its interaction as a substrate rather than nonsubstrate interaction, but that nonsubstrate inhibition by DOX could not be definitely ruled out.

Inhibition of DOX Transport by DNP-SG. Initial velocity of transport was estimated by measuring ATP-dependent DOX uptake at 5 min at five concentrations of DOX between 2 and 6 μM and four concentrations of DNP-SG between 12.5 and 75 μM (25 measurements, each performed in triplicate). Fitting the three variable equation for uncompetitive inhibition (eq 3) yielded a K_{ii} of 19.0 ± 3.4 μM and a reduced χ^2 value of 237, whereas fitting for competitive inhibition (eq 4) yielded a K_{is} of 13.3 ± 2.6 μM and reduced χ^2 value of 108. Fitting the four variable noncompetitive inhibition (eq 5) yielded K_{is} of 16.3 ± 9.8 μM, K_{ii} of 246.0 ± 44.6 μM, and reduced χ^2 of 79. An F test for incremental sum of squares indicated that the precision of the present studies did not justify the inclusion of the additional variable in the analysis (*21*). Eadie–Hofstee plots of the activity data and the theoretical model for competitive inhibition are presented (Figure 9B). This result indicated that inhibition of DOX transport by DNP-SG was more likely due to its interaction as a substrate rather than nonsubstrate interaction, but that nonsubstrate inhibition by DNP-SG could not be definitely ruled out.

DISCUSSION

Our previous studies have suggested that a single transport mechanism, designated as DNP-SG ATPase, could mediate ATP-dependent transport not only of anionic GS-E, but also

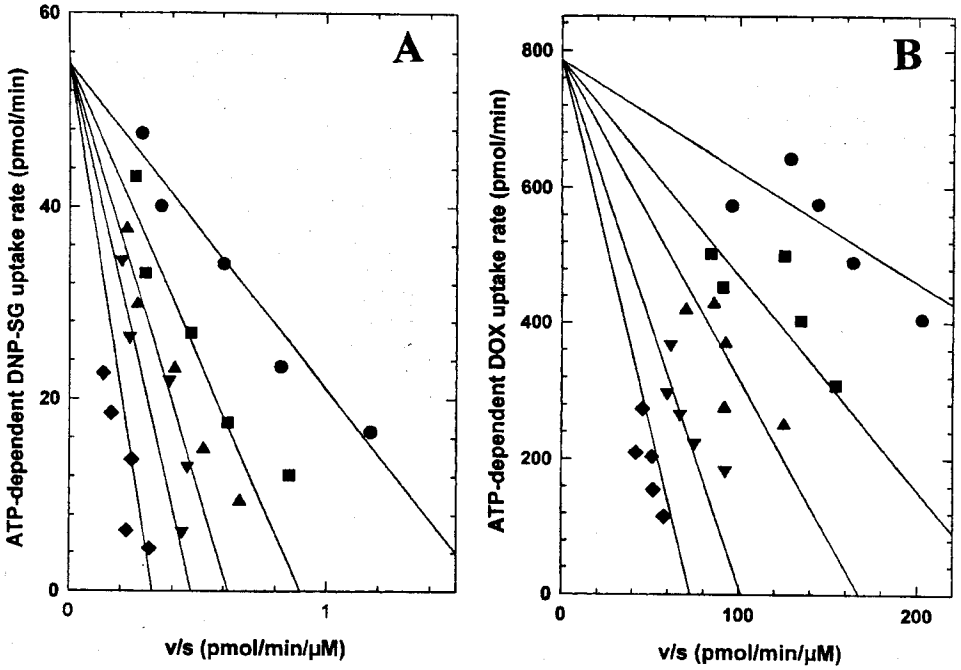

FIGURE 9: Inhibition of ATP-dependent transport of DNP-SG by DOX and of DOX transport by DNP-SG. Proteoliposomes reconstituted with 3 μg of DNP-SG ATPase protein/mL (protein/lipid ratio of 0.6 μg/mg) were diluted 2-fold in transport buffer containing 14, 28, 57, 114, and 170 μM [^{3}H]DNP-SG or 2, 3, 4, 5, and 6 μM 14-[^{14}C]DOX. The effect of DOX at 0 (●), 1 (■), 2 (▲), 3 (▼) or 5 (◆) μM on [^{3}H]DNP-SG transport (panel A) and the effect of DNP-SG at 0 (●), 25 (■), 50 (▼), 75 (▼), or 100 (◆) μM on 14-[^{14}C]DOX transport (panel B) were studied. After equilibration at 37 °C for 10 min, transport was initiated by addition of either 4 mM ATP or 6 mM NaCl. Aliquots of transport buffer (30 μL) were filtered in triplicate after 5 min. Radioactivity remaining on the nitrocellulose filter of each well in the 96 well plate was quantified. ATP-dependent uptake of DNP-SG and DOX was calculated by subtracting uptake in the presence of NaCl from that observed in the presence of ATP. Data are presented as an Eadie-Hofstee plot (v/s vs s, where v is velocity and s is substrate concentration). Points represent average of triplicate determinations with standard deviations less than 5%. The theoretical model was derived from parameters of nonlinear regression for a random bi-bi sequential reaction mechanism (eq 2) to the data.

of weakly basic drugs such as DOX (*6*), which have been shown to be substrates for energy-dependent transport by P-gp (*4*). Because our previous studies (*6*) were carried out in crude erythrocyte membrane vesicles and because the transport of DNP-SG or its inhibition was not directly studied, our previous results did not rule out the possibility that these compounds might be transported by distinct but interrelated transport mechanisms. In the present studies, we have shown functional reconstitution of purified DNP-SG ATPase in artificial liposomes and provided several lines of evidence indicating that DNP-SG ATPase can mediate the ATP-dependent transport of GS-E and DOX.

The presence of ATP resulted in an increased uptake of DOX and DNP-SG in the liposomes reconstituted with active DNP-SG ATPase; the uptake was linear with respect to protein concentration in the vesicles and was saturable with respect to ATP and the other substrate. ADP or methylene ATP could not substitute the function of ATP. ATP-dependent uptake of substrates was shown to be sensitive to temperature with an optimum near 37 °C and declined at higher temperatures, indicating the heat labile nature of the transporter. These results strongly suggest that the transport activity observed in the artificial reconstituted liposomes was due to the presence of a heat labile protein catalyst, rather than due to some nonspecific effect. Present studies also demonstrate that DNP-SG ATPase-mediated ATP-dependent uptake of DOX and DNP-SG in reconstituted vesicle was against a concentration gradient. Analysis of ATP-dependent substrate uptake with resepect to time revealed that uptake could be described reasonably well by a single compartment model consistent with the idea of drug uptake by vesicles mainly into the intravesicular space. The observed K_m for ATP (2.4 mM) was in the range previously observed for Pgp (0.5−1.4 mM) (*4*) and is in the range of physiologic concentration of ATP. Mutual inhibition of transport of DOX and DNP-SG observed during the present studies is consistent with a competitive inhibition model and strongly indicates that both compounds are transported by the same transporter. These lines of evidence strongly suggest that DNP-SG ATPase is a novel membrane ATPase capable of mediating transmembrane movement of small structurally unrelated amphiphilic compounds.

The mutually inhibitory nature of DOX and DNP-SG transport is difficult to reconcile with the binding studies (see the preceding article in this issue), which indicate distinct but possibly spatially related binding sites for DNP-SG and DOX. The binding studies, however, are not strictly comparable with the transport studies since the former were performed in the absence of ATP. Dissimilarity of binding (and perhaps ATPase activating) site for the two compounds does not rule out the presence of a channel common for all substrates into which compounds initally bound at distinct sites are funneled as a result of conformational changes caused by ATP hydrolysis. In preliminary studies, we have obtained a sequence (APAPTPAPAPEXVK) of a peptide fragment obtained from the LYS-C digest of DNP-SG ATPase. Proline-rich sequences such as this are known to be present in channel-forming β-strand domains of other proteins including porins (*22*), α-ketoacid dehydrogenase complex (*23*), and photoreceptor cGMP-gated channel (*24*).

These preliminary results may suggest that DNP-SG ATPase could be a pore-forming protein and the random bi-bi sequential reaction mechanism inferred from kinetic studies is consistent with such an idea. However, further structural studies are necessary before definitive conclusions can be drawn regarding the nature of the transporter and the mechanisms through which it can mediate ATP-dependent transport of anionic DNP-SG as well as weakly cationic amphiphilic compounds such as DOX.

The mechanisms through which a 38 kDa protein, with apparently a much smaller molecular mass than MRP (*17*) or Pgp (*4*, *25*), mediates the transport of structurally diverse compounds with opposite charges need to be investigated. It can be postulated that such a transport may be mediated by as yet uncharacterized channel-forming properties of DNP-SG ATPase particularly in view of the limited sequence information suggesting its homology with porin transmembrane domains (*22*). The determination of complete primary structure of DNP-SG ATPase through its molecular cloning could provide further insight into the mechanisms of transport of compounds with diverse charge and structures by this seemingly unusual transporter and will define its relationship to known organic compound transporting ATPases belonging to the ABC family of proteins such as Pgp or MRP.

Competitive inhibition of the transport of genotoxic amphiphilic xenobiotics by GS-E has some important implications in the fields of carcinogenesis, drug resistance, metabolic modulation of antineoplastic chemotherapy, organ-specific drug toxicity, and idiosyncratic drug toxicity. The number of pharmacologic agents which have minor GS-E metabolites has incresed steadily in recent years. Understanding of potential drug interactions of drugs which form GS-E with genotoxic-xenobiotics or electrophilic drugs used in antineoplastic chemotherapy may offer significant insights into drug interactions and idiosyncratic toxicities as well as strategies for biochemical modulation of chemotherapy.

REFERENCES

1. Kondo, T., Dale, G. L., and Beutler, E. (1981) *Biochim. Biophys. Acta 645*, 132−136.
2. LaBelle, E. F., Singh, S. V., Srivastava, S. K., and Awasthi, Y. C. (1986) *Biochem. J. 238*, 443−449.
3. Kondo, T., Kawakami, Y., Taniguchi, N., and Beutler, E. (1987) *Proc. Natl. Acad. Sci. U.S.A. 84*, 7373−7377.
4. Shapiro, A. B., and Ling, V. (1994) *J. Biol. Chem. 269*, 3745−3754.
5. Schlemmer, S. R., and Sirotnak, F. M. (1994) *J. Biol. Chem. 269*, 31059−31066.
6. Awasthi, S., Singhal, S. S., Srivastava, S. K., Zimniak, P., Bajpai, K. K., Saxena, M., Sharma, R., Ziller, S. A. III, Frenkel, E. P., Singh, S. V., He, N. G., and Awasthi, Y. C. (1994) *J. Clin. Invest. 93*, 958−965.
7. Wei, L. Y., Stutts, M. J., Hoffman, M. M., and Roepe, P. D. (1995) *Biophys. J. 69*, 883−895.
8. Lautier, D., Canitrot, Y., Deeley, R. G., and Cole, S. P. C. (1996) *Biochem. Pharmacol. 52*, 967−977.
9. Loe, D. W., Almquist K. C., Deeley, R. G., and Cole, S. P. C. (1996) *J. Biol. Chem. 271*, 9675−9682.
10. Loe, D. W., Almquist K. C., Cole, S. P. C., and Deeley, R. G. (1996) *J. Biol. Chem. 271*, 9683−9689.
11. Slovak, M. L., Ho, J. P., Cole, S. P. C., Deeley, R. G., Greenberger, L., de Vries, E. G. E., Broxterman, H. J., Scheffer, G. L., and Scheper, R. J. (1995) *Cancer Res. 55*, 4214−4219.
12. Ito, K., Suzuki, H., Hirohashi, T., Kume, K., Shimizu, T., and Sugiyama, Y. (1997) *Am J. Physiol. 272*, G16-G22.
13. Longhurst, T. J., O'Neill, G. M., Harvie, R. M., and Davey, R. A. (1996) *Br. J. Cancer 74*, 1331−1335.
14. Awasthi, S., Singhal, S. S., He, N. G., Chaubey, M., Zimniak, P., Srivastava, S. K., Singh, S. V., and Awasthi, Y. C. (1996) *Int. J. Cancer 68*, 333−339.
15. Allikmets, R., Gerrard, B., Hutchinson, A., and Dean, M. (1996) *Human Mol. Genet. 5*, 1649−1655.
16. LaBelle, E. F., Singh, S. V., Ahmad, H., Wronski, L., Srivastava, S. K., and Awasthi, Y. C. (1988) *FEBS Lett. 228*, 53−56.
17. Cole, S. P. C., Bhardwaj, G., Gerlach, J. H., Mackie, J. E., Grant, C. E., Almquist, K. C., Stewart, A. J., Kurz, E. U., Duncan, A. M. V., and Deeley, R. G. (1992) *Science 258*, 1650−1654.
18. Pikula, S., Hayden, J. B., Awasthi, S., Awasthi, Y. C., and Zimniak, P. (1994) *J. Biol. Chem. 269*, 27574−27579.
19. Miller, C., and Racker, E. (1976) *J. Membr. Biol. 26*, 319−333.
20. Zaman, G. J. R., Lankelma, J., van Tellingen, O., Beijnen, J., Dekker, H., Palusma, C., Oude Elferink, R. P. J., Bass, F., and Borst, P. (1995) *Proc. Natl. Acad. Sci. U.S.A. 92*, 7690−7694.
21. Glantz, S. A. (1990) in *Primer of applied regression and analysis of variance* (Glantz, S. A., and Slinker, B. K., Eds.). McGraw-Hill, Health Professions Divisions, New York, pp 239−271.
22. Jap, B. K., and Walian, P. J. (1996) *Physiol. Rev. 76*, 1073−1088.
23. Meng, M., and Chuang, D. T. (1994) *Biochemistry 33*, 12879−12885.
24. Bureau, M. H., Khrestchatisky, M., Heeren, M. A., Zambrowicz, E. B., Kim, H., Grisar, T. M., Colombini, M., Tobin, A. J., and Olsen, R. W. (1992) *J. Biol. Chem. 267*, 8679−8684.
25. Chin, K. V., Pastan, I., and Gottesman, M. M. (1993) *Adv. Cancer Res. 60*, 157−180.
26. Juliano, R. L., and Ling, V. (1976) *Biochim. Biophys. Acta 455*, 152−162.
27. Horio, M. M., Gottesman, M. M., and Pastan, I. (1988) *Proc. Natl. Acad. Sci. U.S.A. 85*, 3580−3584.

BI972131R